Article

Not peer-reviewed version

Chemical Characteristics and Mechanisms of Nitrate Contamination of Groundwater in Valley Cities in Arid Areas

Linde Liang , Lizhong Zhang , Changli Liu , Jixiang Zhu * , Dun Wang

Posted Date: 24 October 2023

doi: 10.20944/preprints202310.1475.v1

Keywords: hydrochemical characteristics; nitrate; source; valley city

Article

Chemical Characteristics and Mechanisms of Nitrate Contamination of Groundwater in Valley Cities in Arid Areas

Linde Liang [1,2], Lizhong Zhang [3], Changli Liu [1], Jixiang Zhu [1] and Dun Wang [4,*]

[1] Institute of Hydrogeology and Environmental Geology, Chinese Academy of Geological Sciences, Shijiazhuang 050061, China; linde_liang@163.com
[2] China University of Geosciences (Beijing), Beijing 100083, China; linde_liang@163.com
[3] China Geological Survey Comprehensive Survey Command Center for Natural Resources, Beijing 100055, China; Zhanglizhong1015@126.com
[4] Duke Kunshan University, Suzhou 215316, China; wd18856331695@126.com
* Correspondence: hellozjx@126.com

Abstract: With the rapid development of cities in northwest China, there has been an increasing focus on groundwater pollution in plateau cities, specifically the common occurrence of nitrate pollution. The special climatic, geological, and geomorphological characteristics of plateau and river valley cities contribute to distinct groundwater chemical characteristics. Therefore, the formation and evolution process of groundwater nitrate contamination differs from that of plain cities. To explore these issues, we conducted an analysis of eight major ions in various groups of water samples from rivers, springs, and groundwater in Haidong. By utilizing factor analysis and correlation analysis, we were able to identify the characteristics and formation of groundwater chemistry and nitrate pollution in Haidong. Our findings reveal that the chemical characteristics of groundwater in Haidong are primarily controlled by rock weathering, mineral dissolution, and evaporation, leading to the formation of highly mineralized groundwater. Additionally, the excessive nitrate content in certain areas is a result of domestic sewage discharge and agricultural fertilizer use, exceeding Chinese drinking water health standards. Furthermore, for cities located in valleys, the geological structure significantly impacts the nitrate content of groundwater in different regions. Areas with obstructed groundwater flow tend to have higher nitrate levels, while regions with unobstructed groundwater experience lower nitrate concentrations. Notably, shallow groundwater is more vulnerable to nitrate pollution compared to deep groundwater. This study holds great significance in understanding the chemical characteristics of groundwater and the formation and evolution of nitrate pollution in highland river valley cities.

Keywords: hydrochemical characteristics; nitrate; source; valley city

1. Introduction

The scarcity of water resources is currently a pressing issue faced by many countries. Groundwater, as a vital component of freshwater resources, is directly linked to the safety of our drinking water. However, with the progression of the economy and society, groundwater pollution, particularly from nitrate, has become increasingly severe [1]. Nitrate pollution has led to a decline in water quality in numerous countries, significantly impacting the health of residents who rely on drinking water. Elevated levels of nitrate in drinking water pose various health risks, such as methemoglobinemia, gastrointestinal diseases, and blue baby syndrome, thereby increasing the susceptibility to cancer [2–5]. Nitrate exhibits high mobility, and groundwater, characterized by its substantial volume and slow flow rate, serves as a long-term reservoir for nitrate following surface leaching. Over time, the concentration of nitrate in groundwater gradually accumulates [6]. Multiple natural and human-induced factors contribute to nitrate pollution sources. Research has indicated that in rural areas, the leakage of agricultural fertilizers and the discharge of livestock manure are the primary contributors to nitrate pollution [7–9]. However, in urban areas, with the growth of urban populations, the main sources of nitrate pollution have shifted to domestic sewage discharge, landfill

leakage, and nitrate infiltration in urban grasslands, which cannot be overlooked [10–13]. These factors collectively contaminate shallow groundwater. In a study conducted by He [14] in the Yinchuan Plain, a semi-arid region of China, groundwater nitrate pollution was modeled using a random forest approach. The findings revealed that urban land has emerged as a major contributor to nitrate pollution, primarily due to rapid urban development. Furthermore, it is crucial to acknowledge that not only shallow groundwater, but also deep groundwater, which serves as a pathway for pollutants due to deep well exploitation, is contaminated to some extent and poses significant challenges in terms of remediation [15,16].

China is among the countries worldwide that face severe surface and groundwater pollution issues, despite notable progress in water pollution control over the past two decades [17–19]. Nevertheless, new challenges continue to arise, particularly with regard to the increasingly prominent problem of nitrate pollution. Multiple samples have shown nitrate levels surpassing the World Health Organization's drinking water standards (50mg/L), highlighting the urgency of addressing nitrate pollution [20–22]. Controlling nitrate pollution is imperative, as it not only ensures the provision of safe drinking water for residents but is also closely linked to the achievement of sustainable development goals [23]. Currently, the standard limit for nitrate in drinking water in China stands at 44.3 mg/L, considering the existing conditions of nitrate pollution in groundwater. Scholars from around the world have extensively studied the characteristics, sources, migration, transformation, and risk assessment of nitrate pollution [7,16,24,25]. Isotopic methods are frequently employed for identifying the sources and transport of nitrate contamination in groundwater. However, these methods face challenges in accurately reflecting the complex biochemical processes and lagging nature of groundwater [26–28]. Kazakis and Voudouris [16] utilized an improved version of the DRASTIC method, integrating quantitative parameters and modifying the category range and final index of parameters to assess the vulnerability and pollution risk of porous aquifers to nitrate. Building upon the chemical characteristics of groundwater, Xiao et al. [25] investigated the chemical processes occurring in the semi-arid mountain front of northern China and evaluated groundwater risk using the entropy weight water quality index. Dragon et al. [24] employed factor analysis to identify geochemical processes influencing groundwater chemistry, while also examining the influence of aquifer flow systems on groundwater chemistry in Poland's Vilkopolska region. Lahjouj et al. [29] studied the distribution of nitrate in the Quaternary aquifer of the Sais Basin during both spring and fall seasons using statistical methods, discovering that the impact of other chemical components on groundwater nitrate varied between seasons. Additionally, hydrochemistry and isotope tracing methods were employed by Sun et al.[7] to explore the chemical characteristics of groundwater in mountainous regions of North China and assess the influence of lateral recharge on nitrate transport flux. Among these studies, hydrochemistry and multivariate statistical analysis methods were most commonly utilized to uncover the sources and transformation processes of various chemical components within groundwater.

Haidong, located in northwest China along the banks of the Huangshui River, holds significant importance. As a typical valley city, Haidong's groundwater resources are closely tied to its rivers. Unlike most cities, the groundwater flow system in river valley cities primarily centers around the main river valleys within the basin. This unique characteristic facilitates frequent water exchange between groundwater and river water. However, being situated in a plateau area, Haidong exhibits distinct lithological and structural characteristics that differ significantly from those of plain cities. These differences give rise to special recharge and discharge properties of groundwater, further influencing the distribution patterns of pollutants. Over the past few years, the rapid urban development of Haidong has adversely affected its groundwater quality[30,31]. In certain areas, the nitrate content in groundwater exceeds the drinking water standards set by the World Health Organization (50mg/L). This study selects the Ping'an - Ledu Basin in Haidong as the study area, considering its unique geological and geomorphic conditions. By employing hydrogeochemical and multivariate statistical analysis methods, this research endeavors to investigate the chemical characteristics of groundwater, as well as the sources and distribution patterns of nitrate pollution.

Preprints (www.preprints.org) | NOT PEER-REVIEWED | Posted: 24 October 2023 doi:10.20944/preprints202310.1475.v1

2. Study Area

2.1. Physical Geography

The investigated region lies at the junction of the Qinghai-Tibet Plateau and the Loess Plateau, and it is characterized by the Huangshui River passing through the entire study area from west to east (Figure 1), making it a typical valley city. The study area is located at longitudes 101.95 and 102.64 E, and latitudes 36.4 and 36.71 N. The altitude ranges from 1862 m to 4051 m, and it experiences a semi-arid continental climate. The average annual temperature ranges from 0.3 ℃ to 6.8 ℃, with an average annual precipitation of 327.7 mm. Precipitation shows significant spatiotemporal differences, with higher rainfall observed in the mountainous areas to the north and south compared to the central basin. Additionally, precipitation is mainly concentrated between June and September. The study area experiences relatively strong evaporation, with an average annual evaporation of 1580.84 mm. The basin is supplied by multiple tributaries on both the north and south sides, with the Yinsheng River being the largest tributary in terms of water volume and an important water source for Haidong.

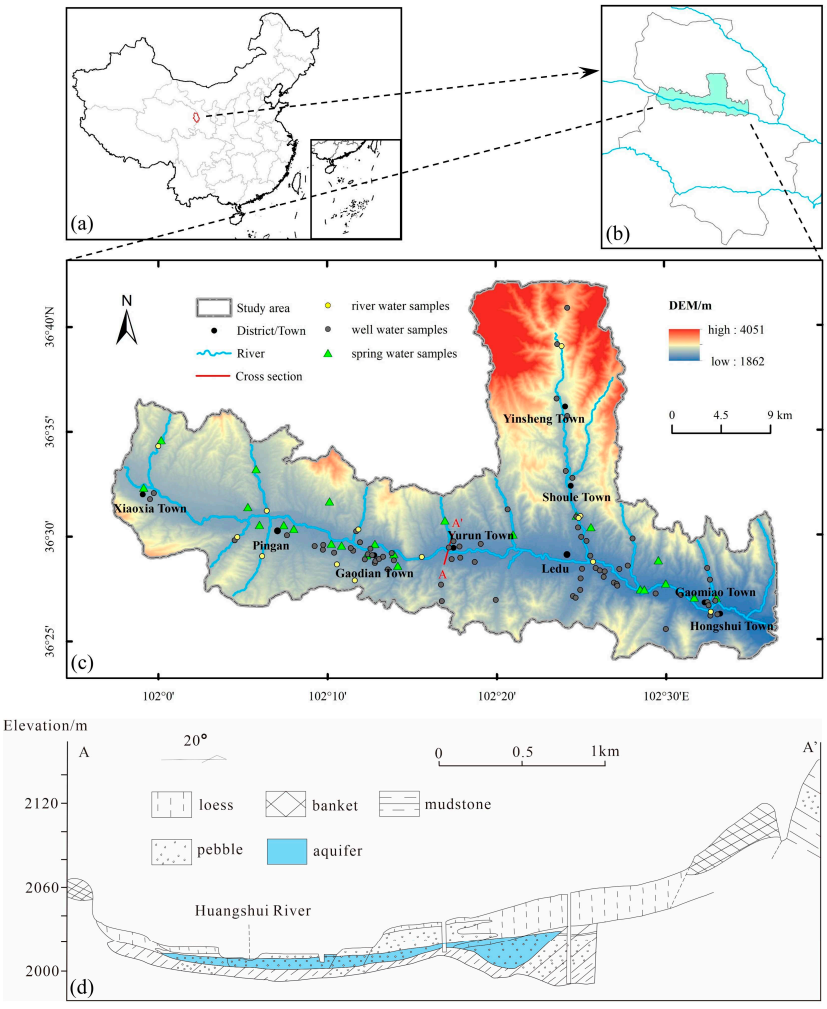

Figure 1. Figure for showing (**a**), (**b**) and (**c**): geographical location, sampling points, and (d): cross section of the study area.

2.2. Geological Conditions

The sedimentary rock layers in the study region consist primarily of three formations, listed from youngest to oldest: (1) The surface is covered with Quaternary loess, with varying thicknesses that gradually increase from the Huangshui River towards the north and south sides, ranging from

Preprints (www.preprints.org) | NOT PEER-REVIEWED | Posted: 24 October 2023 doi:10.20944/preprints202310.1475.v1

2 to 30 meters. (2) Beneath the loess, there is a Quaternary gravel layer that gradually decreases in thickness from the Huangshui River towards the north and south sides, ranging from 3 to 8 meters. This gravel layer serves as the main aquifer in the study area. (3) Underlying the gravel layer are mudstones and sandstones deposited during the Paleogene and Cretaceous periods. Additionally, large deposits of glauberite and gypsum rocks are present. Tectonic activities have had a significant impact on the study area, resulting in the formation of synclinal folds and the Huangshuihe Depression as the main geological structures. Furthermore, local areas exhibit small-scale synclinal water storage structures (Figure 1) due to these tectonic influences.

2.3. Human Activities and Land Use

The study area is situated in the Huangshui River Valley, serving as a significant focal point for both urban and rural communities. In recent years, there has been a considerable increase in urban population, leading to rapid advancements in agriculture and animal husbandry. The land in the area is categorized into seven land use types: grassland, forest land, shrub land, cultivated land, barren land, construction land, and water bodies. Barren land and construction land are primarily found in Ping'an District and Ledu District, the two urban areas. Grassland, forest land, and shrub land are predominantly located in mountainous and hilly regions. Cultivated land is predominantly distributed in the river valley areas on both sides of the Huangshui River and its tributaries, mainly used for growing crops such as wheat, potatoes, and rapeseed. To enhance agricultural production, fertilizers and commercial organic fertilizers are employed in the arable land.

3. Materials and Methods

3.1. Sample Collection and Measurements

A total of 108 groundwater and surface water samples were taken from the study area in 2022, of which groundwater samples included 70 domestic well water samples with a sampling depth of 5-10 m and 25 spring water samples, and 13 surface water samples from the Huangshui River and its tributaries. Well water samples were obtained from wells at a depth of 5-10m, while spring water samples were directly collected from exposed springs. These sampling points were strategically distributed near the Huangshui River and its tributaries, as shown in Figure 1. Upon collection, the samples were analyzed by Qinghai Jiuliu Engineering Exploration and Design Institute. The water chemistry parameters examined in this study included pH, Na+, Ca^{2+}, Mg^{2+}, Cl^-, SO_4^{2-}, HCO_3^-, OH^-, NO_3^-, total dissolved solids (TDS), and total hardness (TH).

To ensure the accuracy and effectiveness of water sample analysis, the ion balance error (E) is calculated using the following formula (Equation (1)):

$$E = \frac{\sum cation - \sum anion}{\sum cation + \sum anion} \times 100\% \quad (1)$$

In Equation (1), the content of anions and cations is expressed in meq/L, and the result of E within ±5% indicates the reliability of the water sample analysis results [32]. The E in this test are all within the range of ±5%, and the water sample testing accuracy is very good.

The remote sensing image dataset and land cover dataset used in this study are respectively from the Geospatial Data Cloud site, Computer Network Information Center of the Chinese Academy of Sciences (https://www.gscloud.cn).

3.2. Correlation Analysis

Correlation analysis is a statistical method utilized to examine the relationship between two or more variables, where correlation coefficients are used to quantify the correlation between these variables. Considering the presence of potential outliers in the chemical parameters of water samples, the Pearson correlation coefficient is deemed unsuitable for this study. Instead, the Spearman correlation coefficient was employed to ascertain the correlation between the following water sample parameters: pH, Na^+, Ca^{2+}, Mg^{2+}, Cl^-, SO_4^{2-}, HCO_3^-, OH^-, NO_3^-, TDS, and TH. When the correlation

Preprints (www.preprints.org) | NOT PEER-REVIEWED | Posted: 24 October 2023 doi:10.20944/preprints202310.1475.v1

coefficient ranges from 0 to 1, it indicates a positive correlation between the variables. Conversely, a correlation coefficient ranging from -1 to 0 signifies a negative correlation. A correlation coefficient of 0 denotes no correlation between the variables. The Spearman correlation coefficient is computed using the formula presented below (Equation (2)).

$$\rho = \frac{\frac{1}{n}\sum_{i=1}^{n}\left(\left(R(x_i)-\overline{R(x)}\right)\left(R(y_i)-\overline{R(y)}\right)\right)\cdot}{\sqrt{\left(\frac{1}{n}\sum_{i=1}^{n}\left(R(x_i)-\overline{R(x)}\right)^2\right)\left(\frac{1}{n}\sum_{i=1}^{n}\left(R(y_i)-\overline{R(y)}\right)^2\right)}} \quad (2)$$

In Equation (2), $R(x)$ and $R(y)$ represent the positions of x and y, respectively, $\overline{R(x)}$ and $\overline{R(y)}$ represent the average positions of x and y, and n represents the total number of samples.

3.3. Factor Analysis

Hidden interconnections frequently exist among different chemical parameters of groundwater. Factor analysis can be employed to categorize these potentially related variables into several independent primary factors, which can effectively demonstrate the associations among the initial variables [18,33]. This approach is commonly used in hydrogeochemistry research, enabling the examination of relationships among various indicators and the determination of hydrogeochemical evolution mechanisms. The modeling process of factor analysis is outlined below.

Assuming that the water sample has a total of p variables X_i (parameter to be analyzed), there is a set of common factors $F_1, F_2, \cdots F_m (m < p)$, and special factors ε_p. Variable X_i, F_m and ε_p satisfy the following model (Equation (3)):

$$\begin{cases} X_1 = \alpha_{11}F_1 + \alpha_{12}F_2 + \cdots + \alpha_{1m}F_m + \varepsilon_1 \\ X_2 = \alpha_{21}F_1 + \alpha_{22}F_2 + \cdots + \alpha_{2m}F_m + \varepsilon_2 \\ \cdots\cdots\cdots \\ X_p = \alpha_{p1}F_1 + \alpha_{p2}F_2 + \cdots + \alpha_{pm}F_m + \varepsilon_p \end{cases} \quad (3)$$

In Equation (3), ε_i is the special factor of X_i, α_{ij} is the load of the i_{th} variable on the j_{ij} factor. The model satisfies the following three assumptions: (1) common factors are not correlated with each other; (2) Special factors are not correlated with each other; (3) There is no correlation between common factors and special factors.

In this study, hydrochemical parameters were used as raw variables to establish an orthogonal factor model. The common factors and factor loading matrix were obtained through principal component analysis, and the factor rotation was performed to determine the significance of each common factor. The factor analysis model is implemented using R 4.3.0.

4. Results and Discussion

4.1. Hydrochemical Characteristics

The statistical results of hydrochemical parameters of collected groundwater and river water samples are shown in Table 1. The levels of ions in groundwater are significantly higher than those in river water. This is largely attributable to the poorer fluidity of groundwater and frequent exchange between river water and other water bodies, which in turn creates higher levels of ions in groundwater. The levels of Na^+ (2.54-2008.59mg/L), K^+ (0-168.92mg/L), SO_4^{2-} (9.61-2713.7mg/L), Cl^- (10.64-3772.25mg/L), and NO_3^- (0-301.6mg/L) vary greatly among different groundwater samples, with CV values of 122.07%, 143.96, 90.36%, 146.31% and 147.77% respectively. However, the changes of HCO_3^- (203.57mg/L-689.53) and pH (7.01-8.3) were small in both groundwater and river water, and the water samples in the study area were alkaline. The consentration of SO_4^{2-}, TDS (235.29-9235.48 mg/L) and TH (230.18-3522.82 mg/L) in groundwater are typically elevated, with more than 50% of the samples surpassing the Chinese drinking water hygiene standards. Furthermore, certain groundwater samples exhibit NO_3^- concentrations that significantly exceed the Chinese standard for drinking water hygiene. The pH of groundwater ranges from 7.01 to 8.26, which falls within the 6.5-8.5 range stipulated by Chinese drinking water standards.The adbundance of cation in groundwater

Preprints (www.preprints.org) | NOT PEER-REVIEWED | Posted: 24 October 2023 doi:10.20944/preprints202310.1475.v1

is ranked: Na^+>Ca^{2+}>Mg^{2+}>K^+, and the adbundance of annion in groundwater is ranked: SO_4^{2-}>HCO_3^->Cl^->NO_3^-.

Table 1. Results of hydrochemical analysis.

Parameters	Units	Maximum		Minimum		Mean		Median		CV		standard
		GW	SW	GW	SW	GW	SW	GW	SW	GW	SW	
Na^+	mg/L	2008.6	476.3	2.54	4.04	249.2	157.8	159.4	81.1	122.1%	95.5%	200
K^+	mg/L	168.9	56.3	0	0	21.9	13.2	9.9	5.1	144%	130.4%	/
Ca^{2+}	mg/L	571.1	288.58	36.1	52.1	211.3	128.4	180.4	91.2	57.6%	58.3%	/
Mg^{2+}	mg/L	509.1	104.49	0	15.8	92.5	53.3	76.6	45.6	78.9%	61.1%	/
Cl^-	mg/L	3722.3	506.94	14.2	10.64	308.1	168.4	198.5	85.1	146.3%	100.1%	250
SO_4^{2-}	mg/L	2713.7	1068.7	9.6	38.42	636.1	389.8	446.7	266.6	90.4%	88.9%	250
HCO_3^-	mg/L	689.5	378.32	203.6	201.37	403.6	267.5	408.8	256.3	24.2%	18.3%	/
NO_3^-	mg/L	301.1	77.96	0	5.39	29.3	21.1	11.3	15.4	147.8%	89.8%	44.3
pH	/	8.3	8.26	7.01	7.21	7.5	7.9	7.5	8.1	3.45%	4.3%	6.5-8.5
TDS	mg/L	9235.5	2346.6	278.1	235.29	1714.3	1032.8	1349	698.2	80.6%	75.8%	1000
TH	mg/L	3522.8	1105.9	230.2	210.17	909.5	540	840.7	445.4	60.8%	57%	450

[1] GW: groundwater.; SW: surface water; CV: coefficient of variation.[2] Standard: Standard for Drinking Water develped by China (GB 5749-2022).

Based on the diagram of The Piper (1944) (Figure (2)), the chemical composition of the groundwater samples can be categorized into three types: HCO_3-SO_4-Cl-Ca-Na, HCO_3-SO_4-Ca-Mg, and SO_4-Na. Similarly, the chemical composition of the river water samples can be classified into two types: HCO_3-SO_4-Cl-Ca-Na and HCO_3-SO_4-Ca-Na. It is worth noting that the chemical composition of the river closely resembles that of the groundwater. This can be attributed to the fact that the rivers in the study area are primarily fed by groundwater discharge, with the exception of specific storage areas. Moreover, the rivers receive additional recharge from surface runoff, which chemically resembles precipitation and has relatively low ion levels. Consequently, the chemical composition of river water is comparatively lower than groundwater. Interestingly, more than half of the groundwater samples exhibited high total dissolved solids (TDS) due to significantly elevated levels of SO_4^{2-}, Cl^-, and Na^+. As a result, certain regions within the study area have highly mineralized groundwater.

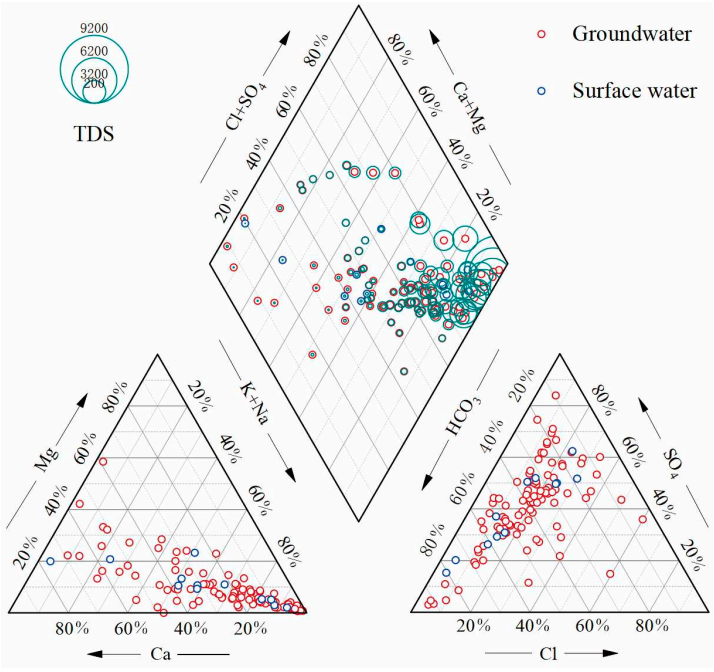

Figure 2. Piper diagram shouwing the chemical of groundwater samples and surface water samples.

Preprints (www.preprints.org) | NOT PEER-REVIEWED | Posted: 24 October 2023 doi:10.20944/preprints202310.1475.v1

According to the distribution of each chemical constituent (Figure (3)), groundwater with high TDS is primarily found on the periphery of river valleys. This particular groundwater exhibits a chemical composition dominated by SO_4^{2-}, Cl^-, and Na^+. Conversely, HCO_3^-, Ca^{2+}, and Mg^{2+} are relatively evenly distributed in the water samples and serve as the main ionic components in groundwater with low TDS. These low TDS groundwater sources are primarily found along rivers. The distribution of NO_3^- displays regional variations, with higher concentrations observed in the western part of the study area compared to the eastern part. In fact, more than half of the water samples in the western region exceeded the Chinese drinking water standard for NO3-. However, in the eastern region, a majority of the water samples complied with the Chinese drinking water standard for NO_3^-. Nonetheless, sporadic occurrences of high NO_3^- levels exceeding the Chinese drinking water standards were observed in certain areas within the groundwater distribution.

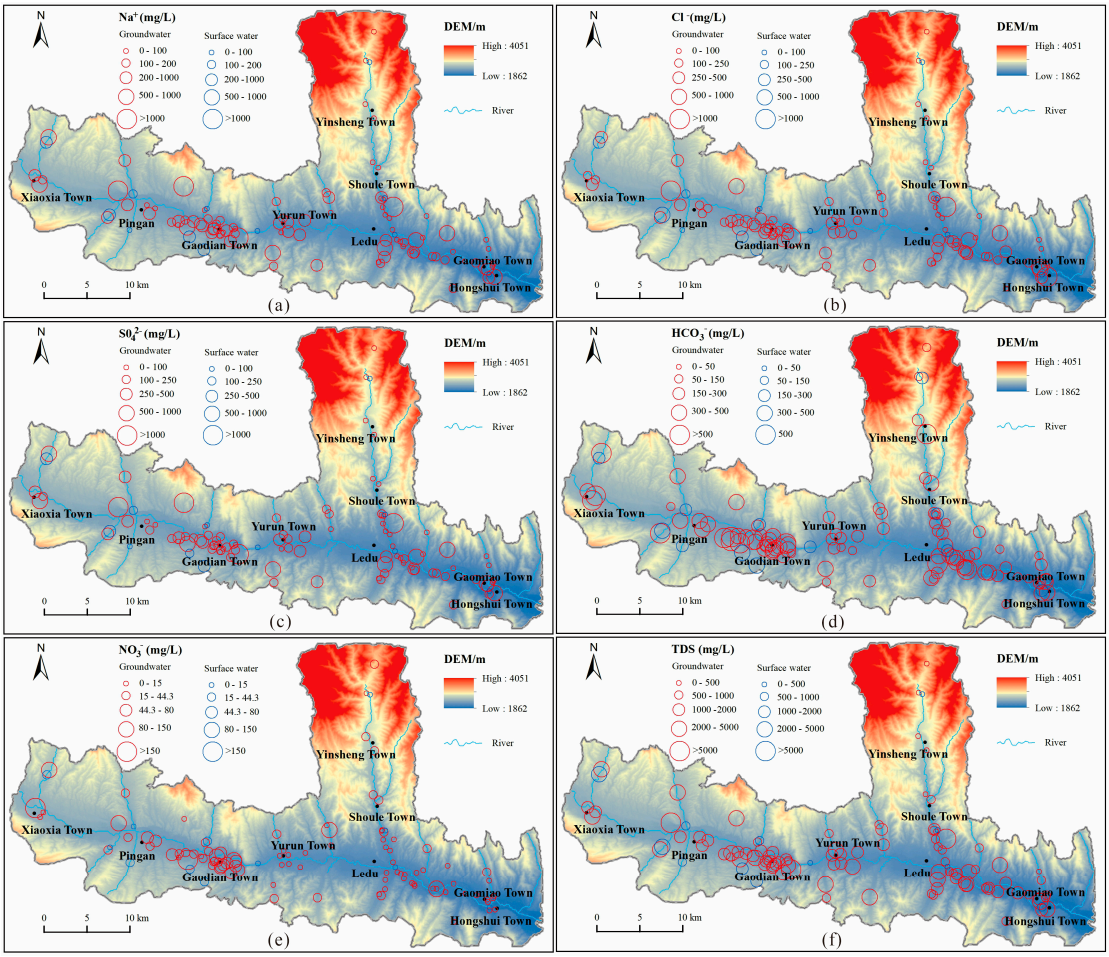

Figure 3. Distribution of chemical constituents in groundwater samples and surface water samples.

4.2. Result of Factor Analysis

Factor analysis was conducted on the groundwater samples in the study area, targeting the eight major ionic constituents. Factor rotation was applied to obtain three principal factors (Table 2). Among these factors, F1 exhibited a significant correlation with Na^+ and Cl^- with a factor contribution of 28.9%. Conversely, F1 displayed weak correlation with Ca^{2+} and a negative correlation with HCO_3^-. This pattern can be attributed to evapotranspiration, which results in elevated levels of Na^+ and Cl^-, while HCO_3^- and Ca^{2+} precipitate after reaching their saturation concentrations. F2 accounted for 26.7% of the variability and exhibited strong correlation with Ca^{2+} and SO_4^{2-}, while displaying relatively weak correlations with Na^+, K^+, and Cl^-. This can be attributed to the fact that F2 predominantly reflects rock weathering and the dissolution of minerals such as mirabilite and gypsum. F3 contributed 10.6% and demonstrated high correlation with Mg^{2+}, HCO_3^-, and NO_3^-. In

Preprints (www.preprints.org) | NOT PEER-REVIEWED | Posted: 24 October 2023 doi:10.20944/preprints202310.1475.v1

contrast, it showed no correlation with Na^+ and K^+. F3 is likely associated with carbonate rock dissolution and human activities. The first two factors exhibited similar contribution rates and are primarily determined by climatic and geological conditions, representing the main factors influencing the chemical composition of groundwater. On the other hand, the third factor is primarily linked to groundwater pollution by sewage and agricultural effluent discharges.

Table 2. Table of principal component rotation variable.

Original variable	Load of each principal component variable		
	F1	F2	F3
Na^+	0.801	0.541	0.000
K^+	0.486	0.284	0.000
Ca^{2+}	0.342	0.767	0.145
Mg^{2+}	0.513	0.490	0.701
Cl^-	0.929	0.281	0.229
SO_4^{2-}	0.344	0.913	0.209
HCO_3^-	-0.211	0.144	0.282
NO_3^-	0.157	0.000	0.380
Eigenvalue	2.311	2.140	0.846
Contribution of variance/%	28.9	26.7	10.6
Cumulative contribution/%	28.9	55.6	66.2

It can be observed that SO_4^{2-} and Ca^{2+} exhibit strong positive correlation, with similar loadings across all three principal components. This suggests that these two ions share the same source, with only a small portion exhibiting different sources (Figure (4)). Na^+ and Cl^- also display a strong correlation, but Na^+ has higher loadings for F2, while Cl^- has higher loadings for F3. However, only HCO_3^- demonstrates a negative loading on F1 compared to the other ions. This implies that HCO_3^- has reached a saturated concentration in the groundwater within the study area, and its concentration cannot be further increased through evaporation. The higher loading of NO_3^- on both F1 and F3, together with its very low loading on F2, reflects the fact that NO_3^- in groundwater is primarily influenced by human activities and evapotranspiration, rather than mineral dissolution.

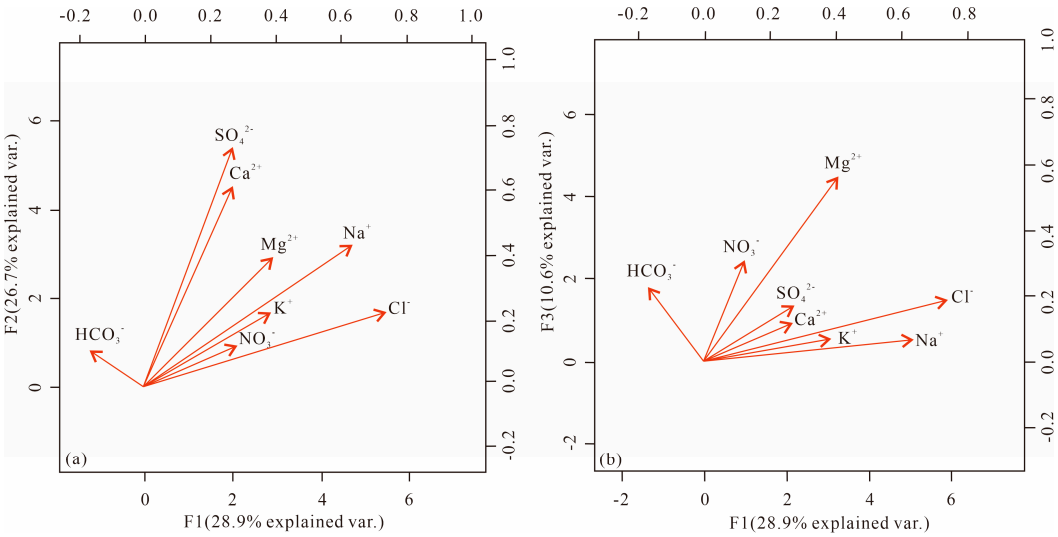

Figure 4. Plot of information on each principal component.

4.3. Mechanism Controlling Water Chemistry

The formation of groundwater chemical characteristics is influenced by various factors, such as stratigraphic lithology, geological formations, climatic factors, and human activities. Gibbs [34] classified the mechanisms of hydrochemical formation in their natural state into three categories: rock

Preprints (www.preprints.org) | NOT PEER-REVIEWED | Posted: 24 October 2023 doi:10.20944/preprints202310.1475.v1

weathering, evaporation, and atmospheric precipitation. Based on this classification, Gibbs developed a semi-logarithmic plot representation. In this study, the Gibbs diagram was employed to identify the dominant factors contributing to the formation of groundwater chemistry features in the study area (Figure 5a). It is evident that the chemical characteristics of groundwater in the study area are primarily influenced by rock weathering and evapotranspiration. Conversely, the impact of precipitation on groundwater chemistry is minimal, aligning with the region's low precipitation levels as previously indicated.

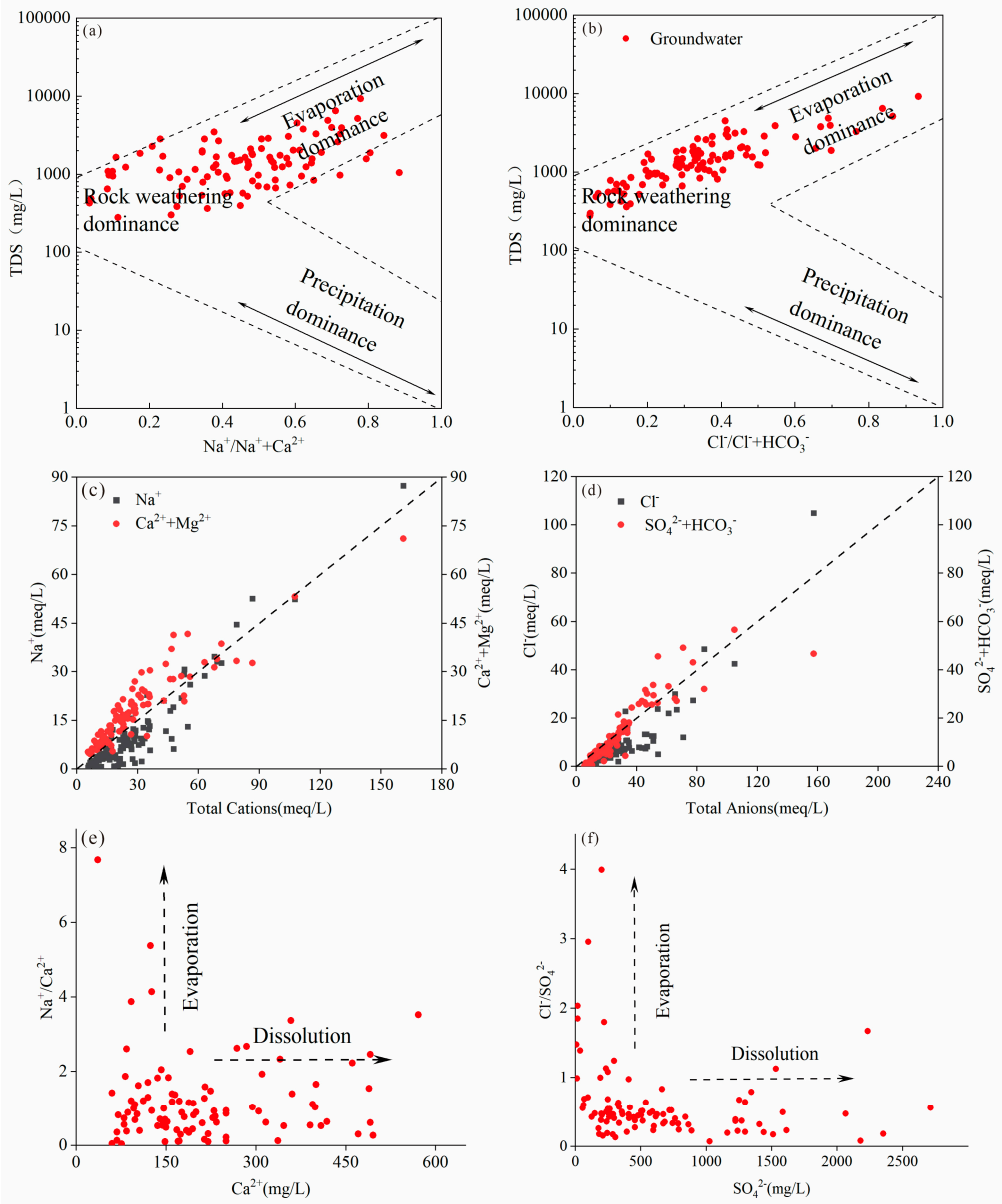

Figure 5. The relationship between ions: (a) and (b) gibbs diagram indicating factors controlling the chemical characteristics of groundwater, (c) Na^+, Ca^{2+}+Mg^{2+} vs Total Cations (meq/L), (d) Cl^-, SO_4^{2-} +HCO_3^- vs Total Anions (meq/L), (e) Na^+/Ca^{2+} vs Ca^{2+}(mg/L) and (f) Cl^-/SO_4^{2-} vs SO_4^{2-}(mg/L).

4.3.1. Rock Weathering

Weathering of rocks and mineral dissolution are the primary sources of various chemical constituents in groundwater [35]. As illustrated in Figure 5a,b, rock weathering and mineral dissolution are found to play a dominant role in the formation of groundwater chemical characteristics. Correlation analysis results (Table 3) indicate a significant correlation between Na^+ and Cl^- as well as SO_4^{2-}. Additionally, strong correlation between Ca^{2+} and SO_4^{2-} is observed.

Preprints (www.preprints.org) | NOT PEER-REVIEWED | Posted: 24 October 2023 doi:10.20944/preprints202310.1475.v1

Furthermore, HCO_3^- exhibits correlation solely with Ca^{2+} and Mg^{2+}, with limited association with other ions. This suggests that the dissolution of dolomite, gypsum, halite, and thenardite in the study area is likely responsible for these correlations. The red layer, which contains a considerable amount of gypsum, thenardite, halite, and some dolomite, is widely distributed in the stratigraphy of the study area. These minerals dissolve in groundwater, and the reaction process is represented by the following equation:

$$CaSO_4 \cdot 2H_2O \rightarrow Ca^{2+} + SO_4^{2-} + 2H_2O \quad (4)$$

$$Na_2SO_4 \rightarrow 2Na^+ + SO_4^{2-} \quad (5)$$

$$NaCl \rightarrow Na^+ + Cl^- \quad (6)$$

$$CaMg(CO_3)_2 + 2H_2O \rightarrow Ca^{2+} + Mg^{2+} + 2HCO_3^- + 2OH^- \quad (7)$$

Table 3. Correlation coefficient of major ions.

Index	Na^+	K^+	Ca^{2+}	Mg^{2+}	Cl^-	SO_4^{2-}	HCO_3^-	NO_3^-
Na^+	1							
K^+	0.5756	1						
Ca^{2+}	0.5999	0.3543	1					
Mg^{2+}	0.7325	0.4487	0.6499	1				
Cl^-	0.9154	0.5499	0.5738	0.7752	1			
SO_4^{2-}	0.7879	0.4445	0.8524	0.7706	0.6240	1		
HCO_3^-	0.0002	0.0176	0.1684	0.1604	-0.0965	0.1136	1	
NO_3^-	0.2418	0.1943	0.2161	0.3844	0.2519	0.1992	0.3879	1

As shown in Figure 5c,d, when the TDS is high, the content of SO_4^{2-} in groundwater is superior to that of Ca^{2+} and Mg^{2+}, and the concentration of SO_4^{2-} and Cl^- is very high. As shown in Figure 5e and 5f, The formation of large amounts of Ca^{2+} and SO_4^{2-} contained in groundwater in the study area is contributed to rock weathering and mineral dissolution, and the concentration of SO_4^{2-} is slightly higher than the concentration of Ca^{2+}. After analyzing the solubility of several minerals (Figure 6a), we found that the SI of dolomite and gypsum in the study area is greater than 0, indicating that both minerals are in a saturated state and Ca^{2+} in groundwater cannot continue to increase. The SI of thenardite is less than 0, indicating that thenardite in groundwater is not yet saturated and is in a dissolved state and SO_4^{2-} in groundwater can continue to increase. Therefore, the concentration of SO_4^{2-} in groundwater is higher than that of Ca^{2+}. In addition, besides thenardite, the SI of halite is also less than 0, which is in a dissolved state, leading to a continuous increase in the content of SO_4^{2-}, Na^+, and Cl^- in groundwater. Therefore, these three ions are the main ions in highly mineralized groundwater.

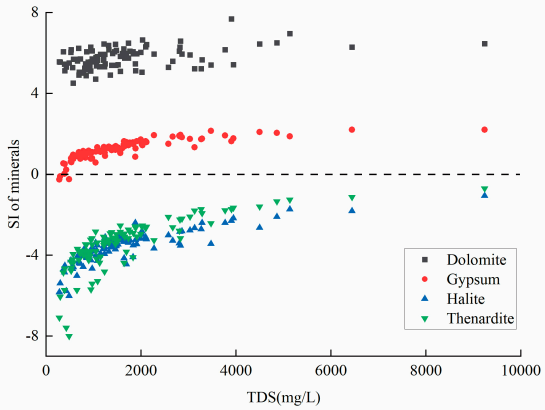

Figure 6. Variation of saturation indices of several minerals.

 doi:10.20944/preprints202310.1475.v1

4.3.2. Evaporation

Evaporation is an important driving force controlling the formation of chemical characteristics of groundwater [36]. The altitude of the study area is very high, in the range of 1862 m-4051 m, which leads to very strong lighting in the study area. And the groundwater table in the study area is very shallow, in the range of 1 m-10 m. The depth to the groundwater table in the study area is very shallow, in the range of 1 to 10 m, and due to the high altitude, which in turn leads to strong evaporation of groundwater. Due to the poor mobility of groundwater, affected by evaporation, various ions continue to dissolve, the concentration increases. Under the influence of these two factors, the evaporation of groundwater in the study area is very strong, and the precipitation in the study area is significantly lower than the evaporation, resulting in an increase in ion concentration in areas with poor groundwater mobility, leading to the formation of highly mineralized groundwater.

4.4. Analysis of the Origin of Nitrates

Based on the distribution of nitrate content in groundwater (Figure 7), we observed a distinct pattern within the study area (Xiaoxia, highlighted in the red box in Figure 7a). In this area, the nitrate concentration in groundwater on the western side was significantly higher, with a majority of water samples exceeding Chinese drinking water standards. However, on the eastern side of the area, the nitrate concentration in most groundwater samples was considerably lower, well below the Chinese drinking water standards. Upon analyzing the relationship between nitrate distribution in groundwater and land use types, we found that the groundwater with high nitrate concentration in the western part of the study area primarily originates from agricultural and residential areas situated within river valleys. Notably, no industrial wastewater generated by factories was found in this area. Conversely, the nitrate concentration in groundwater was low in the agricultural areas located in the eastern part of the study area. This suggests that agricultural activities and domestic wastewater likely contribute to the orgin of nitrate in groundwater. However, it is evident that other factors besides these also play a role in the formation of high concentrations of nitrate in groundwater.

Further analysis of the lithology and geological structure of the study area's inner strata reveals the presence of metamorphic rocks in the shallow layers in Xiaoxia. In contrast, pebble layers cover the shallow strata in other areas. As metamorphic rocks are impermeable, they act as barriers to the phreatic aquifer, preventing any connection between the groundwater on either side. The aquifer located upstream on the west side of Xiaoxia poses difficulties for the downward flow and discharge of groundwater. Instead, groundwater primarily gets discharged through the Huangshui River and evaporation. Consequently, nitrate generated by agricultural activities has limited mobility into the groundwater. With evaporation, the concentration of nitrate in groundwater steadily increases, leading to the formation of high-concentration nitrate groundwater. In comparison, the aquifer on the east side of Xiaoxia is situated downstream, facilitating unobstructed groundwater flow. Nitrate enters the groundwater and gets discharged downstream through runoff, making it challenging to develop groundwater with high nitrate concentration.

Preprints (www.preprints.org) | NOT PEER-REVIEWED | Posted: 24 October 2023 doi:10.20944/preprints202310.1475.v1

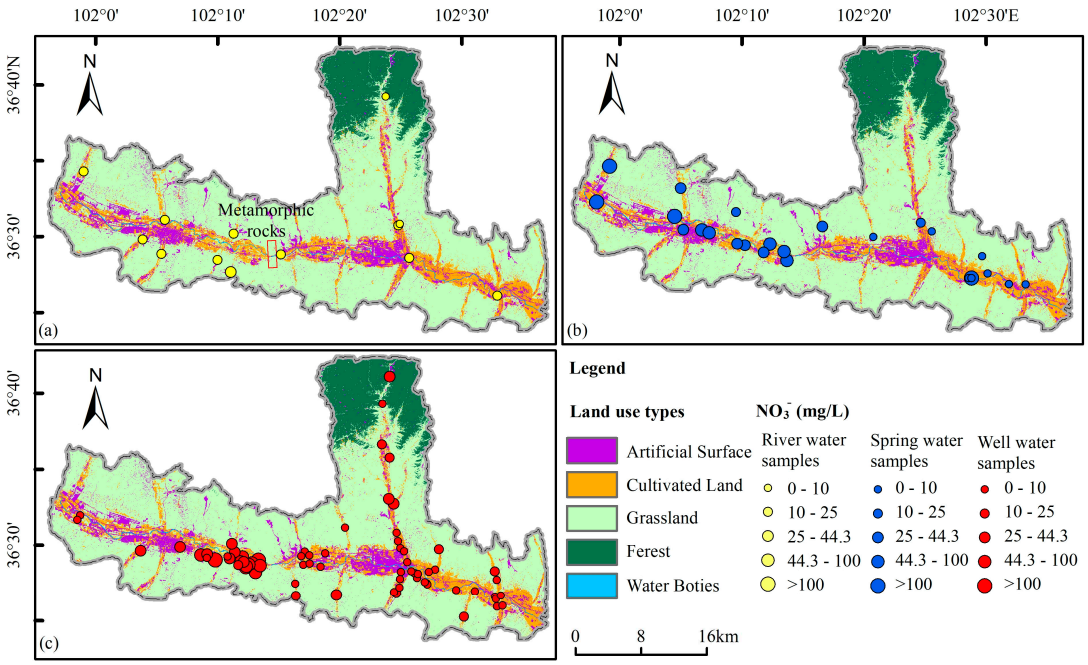

Figure 7. Distribution of NO_3^- and land use types: (**a**) NO_3^- in surface water, (**b**) NO_3^- in spring water and (**c**) NO_3^- in well water.

Considering the stable bicarbonate content of groundwater in the study area, we conducted an analysis of the relationship between NO_3^-/HCO_3^- and $(Cl^-+SO_4^{2-})/HCO_3^-$ in the samples of spring and well water (Figure 8). We found that the spring water had significantly higher NO_3^- content compared to the well water. This disparity can primarily be attributed to the thin overlying vadose zone near the spring site, which allows pollutants from the surface such as agricultural fertilizers, leakage from landfill site and domestic sewage to infiltrate the aquifer more easily, resulting in elevated levels of NO_3^- in the spring water. In contrast, the vadose zone of the well water from deeper depths is thicker and offers greater resistance to pollutants. Furthermore, the upper portion of the aquifer in the study area consists of a layer of loess, while the soluble sedimentary rocks are located in the lower part of the aquifer. As a result, the chemical characteristics of the well water at deeper depths are more significantly influenced by rock weathering and mineral dissolution so that there are higher levels of Cl^- and SO_4^{2-} in well water than in spring water.

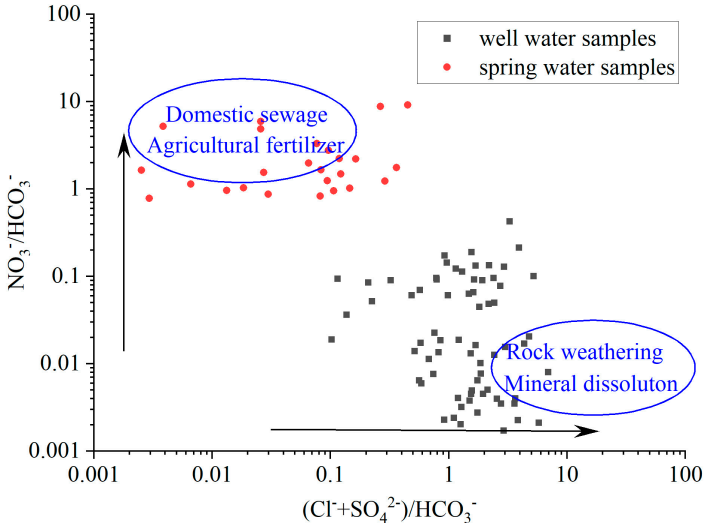

Figure 8. Plot of NO_3^-/HCO_3^- vs $(Cl^-+SO_4^{2-})/HCO_3^-$ of groundwater.

5. Conclusions

Valley cities in arid areas are influenced by their unique geological and climatic conditions, leading to distinct chemical characteristics of groundwater and pollutant transport compared to the cities situated in plain. In Haidong, it was found that a significant number of soluble rocks buried in the strata served as soluble sources. Additionally, the low precipitation and high evaporation rates in the study area contributed to the generally high TDS content in groundwater.

The contamination of groundwater with nitrate in the study area is mainly attributed to the agricultural and residential areas. Agricultural fertilizers, livestock manure, leakage from landfill site and domestic pollution discharges are the primary sources. However, due to the development of folding, the valley cities have distinct geological and geomorphological conditions that can result in aquifer blockage by insoluble rocks. This limits the connectivity between upstream and downstream groundwater, causing nitrate to accumulate in higher concentrations in the upstream groundwater while exhibiting lower nitrate levels in downstream aquifers with smoother water flow. Therefore, when addressing groundwater pollution issues in valley cities, it is crucial to consider whether geological structural factors have hindered the flow of groundwater, making it difficult to discharge and leading to the accumulation of pollutants. In tackling such problems, manual methods can be utilized, such as removing obstacles or constructing underground water pipelines, to establish connectivity between both sides of the aquifer. These approachs can enhance the mobility of underground water flow and reduce the concentration of pollutants.

Moreover, the depth of groundwater burial varies across the study area, leading to areas with shallow water tables being more susceptible to nitrate contamination, while deeper groundwater remains relatively safer. We are sopposed to strengthen the protection of shallow groundwater.

Author Contributions: Methodology, investigation, writing-original draft, L.D.-L; review & supervision, L.Z.-Z.; review & supervision, C.L.-L.; review & supervision, J.X.-Z.; software & supervision, D.-W..

Funding: This study was supported by a grant from the Urban Geological Survey of Haidong City, Qinghai Province, China (No. Q202217).

Data Availability Statement: Data will be made available on request.

Conflicts of Interest: The authors declare no conflict of interest.

References

1. Abbasnia, A.; Yousefi, N.; Mahvi, A. H.; Nabizadeh, R.; Radfard, M.; Yousefi, M.; Alimohammadi, M. Evaluation of groundwater quality using water quality index and its suitability for assessing water for drinking and irrigation purposes: Case study of Sistan and Baluchistan province (Iran). *Hum. Ecol. Risk Assess.* **2019,** 25, 988-1005.
2. Li, R. Development and performance study of in-situ bioremediation simulation device for nitrate pollution in groundwater. China University of Geosciences (Beijing). 2015.
3. Qasemi, M.; Farhang, M.; Morovati, M.; Mahmoudi, M.; Ebrahimi, S.; Abedi, A.; Bagheri, J.; Zarei, A.; Bazeli, J.; Afsharnia, M.; Ghalehaskar, S.; Ghaderpoury, A. Investigation of potential human health risks from fluoride and nitrate via water consumption in Sabzevar, Iran. *Int. J. Environ. Anal. Chem.* **2022,** 102, 307-318.
4. Xin, J.; Wang, Y.; Shen, Z. L.; Liu, Y.; Wang, H. T.; Zheng, X. L. Critical review of measures and decision support tools for groundwater nitrate management: A surface-to-groundwater profile perspective. *J. Hydrol.* **2021,** 598, 126386.
5. Zhang, Q. Q.; Wang, H. W.; Wang, L. Tracing nitrate pollution sources and transformations in the over-exploited groundwater region of North China using stable isotopes. *J. Contam. Hydrol.* **2018,** 218, 1-9.
6. Woodward, S. J. R.; Stenger, R.; Bidwell, V. J. Dynamic analysis of stream flow and water chemistry to infer subsurface water and nitrate fluxes in a lowland dairying catchment. *J. Hydrol.* **2013,** 505, 299-311.
7. Sun, R. B.; Ding, J. K.; Li, H. Y.; Wang, X. G.; Li, W. Y.; Li, K. X.; Ye, X. X.; Sun, S. Y. Mitigating nitrate leaching in cropland by enhancing microbial nitrate transformation through the addition of liquid biogas slurry. *Agric. Ecosyst. Environ.* **2023,** 345.
8. Chen, R. D.; Hu, Q. H.; Shen, W. Q.; Guo, J. X.; Yang, L.; Yuan, Q. Q.; Lu, X. M.; Wang, L. C. Identification of nitrate sources of groundwater and rivers in complex urban environments based on isotopic and hydro-chemical evidence. *Sci. Total Environ.* **2023,** 871, 162026.

9. Cao, X.; Shi, Y. Y.; Wei, H.; An, T. Y.; Chen, X. R.; Zhang, Z. H.; Liu, F.; Zhao, Y.; Zhou, P. P.; Chen, C. B.; He, J. T.; He, W. Impacts of anthropogenic groundwater recharge (AGR) on nitrate dynamics in a phreatic aquifer revealed by hydrochemical and isotopic technologies. *Sci. Total Environ.* **2022,** 839, 156187.
10. Adimalla, N.; Qian, H. Groundwater chemistry, distribution and potential health risk appraisal of nitrate enriched groundwater: A case study from the semi-urban region of South India *Ecotoxicol. Environ. Saf.* **2021,** 207, 111277.
11. Gu, B.; Ge, Y.; Chang, S.; Luo, W.; Chang, J. Nitrate in groundwater of China: Sources and driving forces. *Global Environ. Change Part A: Hum. & Policy Dimens.* **2013,** 23, 1112-1121.
12. Panahi, G.; Eskafi, M. H.; Rahimi, H.; Faridhosseini, A.; Tang, X. N. Physical–chemical evaluation of groundwater quality in semi-arid areas: case study—Sabzevar plain, Iran. *Sustain. Water Resour. Manage.* **2021,** 7.
13. Zhai, Y.; Zheng, F.; Zhao, X.; Xia, X.; Teng, Y. Identification of hydrochemical genesis and screening of typical groundwater pollutants impacting human health: A case study in Northeast China(Article). *Environ. Pollut.* **2019,** 252, 1202-1215.
14. He, S.; Wu, J. H.; Wang, D.; He, X. D. Predictive modeling of groundwater nitrate pollution and evaluating its main impact factors using random forest. *Chemosphere.* **2022,** 290, 133388.
15. Han, D. M.; Currell, M. J.; Cao, G. L. Deep challenges for China's war on water pollution. *Environ.Pollut.* **2016,** 218, 1222-1233.
16. Kazakis, N.; Voudouris, K. S. Groundwater vulnerability and pollution risk assessment of porous aquifers to nitrate: Modifying the DRASTIC method using quantitative parameters. *J. Hydrol.* **2015,** 525, 13-25.
17. Feng, W. W.; Wang, C.; Lei, X. H.; Wang, H.; Zhang, X. L. Distribution of nitrate content in groundwater and evaluation of potential health risks: A case study of rural areas in northern China *Int. J. Environ. Res. Public Health.* **2020,** 17, E9390.
18. Liu, L. N.; Wu, J. H.; He, S.; Wang, L. Occurrence and distribution of groundwater fluoride and manganese in the Weining Plain (China) and their probabilistic health risk quantification. *Exposure Health.* **2022,** 14, 263-279.
19. Tang, W. Z.; Pei, Y. S.; Zheng, H.; Zhao, Y.; Shu, L. M.; Zhang, H. Twenty years of China's water pollution control: Experiences and challenges. *Chemosphere.* **2022,** 295, 133875.
20. Wen, X. H.; Feng, Q.; Lu, J.; Wu, J.; Wu, M.; Guo, X. Y. Risk assessment and source identification of coastal groundwater nitrate in northern China using dual nitrate isotopes combined with Bayesian mixing model. *Hum. Ecol. Risk Assess.* **2018,** 24, 1043-1057.
21. Wu, J.; Zhao, W. D.; Lu, J.; Jin, S.; Wang, J. Q.; Qian, J. Z. Geographic information system based approach for the investigation of groundwater nitrogen pollution near a closed old landfill site in beijing, China. *Environ. Eng. Manag. J.* **2018,** 17, 1095-1101.
22. Zhang, X.; Zhang, Y.; Shi, P.; Bi, Z. L.; Shan, Z. X.; Ren, L. J. The deep challenge of nitrate pollution in river water of China. *Sci. Total Environ.* **2021,** 770, 144674.
23. Wang, M.; Janssen, A. B. G.; Bazin, J.; Strokal, M.; Ma, L.; Kroeze, C. Accounting for interactions between Sustainable Development Goals is essential for water pollution control in China. *Nat. Commun.* **2022,** 13, 730.
24. Dragon, K.; Gorski, J. Identification of groundwater chemistry origins in a regional aquifer system (Wielkopolska region, Poland. *Environ. Earth Sci.* **2015,** 73, 2153-2167.
25. Xiao, Y.; Liu, K.; Hao, Q. C.; Xiao, D.; Zhu, Y. C.; Yin, S. Y.; Zhang, Y. H. Hydrogeochemical insights into the signatures, genesis and sustainable perspective of nitrate enriched groundwater in the piedmont of Hutuo watershed, China. *Catena.* **2022,** 212, 106020.
26. Erostate, M.; Huneau, F.; Garel, E.; Lehmann, M. F.; Kuhn, T.; Aquilina, L.; Vergnaud-Ayraud, V.; Labasque, T.; Santoni, S.; Robert, S.; Provitolo, D.; Pasqualini, V. Delayed nitrate dispersion within a coastal aquifer provides constraints on land_use evolution and nitrate contamination in the past. *Sci.Total Environ.* **2018,** 644, 928-940.
27. Nestler, A.; Berglund, M.; Accoe, F.; Duta, S.; Xue, D.; Boeckx, P.; Taylor, P. Isotopes for improved management of nitrate pollution in aqueous resources: review of surface water field studies. *Environ. Sci. Pollut. R.* **2011,** 18, 519-533.
28. Taufiq, A.; Effendi, A. J.; Iskandar, I. Controlling factors and driving mechanisms of nitrate contamination in groundwater system of Bandung Basin, Indonesia, deduced by combined use of stable isotope ratios, CFC age dating, and socioeconomic parameters. *Water Res* **2019,** 148, 292-305.
29. Lahjouj, A.; El Hmaidi, A.; Bouhafa, K. Spatial and statistical assessment of nitrate contamination in groundwater: Case of sais basin, Morocco. *J. Groundwater Sci. Eng.* **2020,** 8, 143-157.
30. Jiao, Z. R. Research on Evolution of Groundwater ChemicalCharacteristics of Ledu basin in the Eastern Qinhai Province. Hebei University of Geosciences, China, 2018.
31. Liu, Q. The groundwater chemical characteristics in Ping'an basin in east Qinghai province. Hebei University of Geosciences, China, 2018.

32. Su, H.; Kang, W. D.; Li, Y. R.; Li, Z. Fluoride and nitrate contamination of groundwater in the Loess Plateau, China: Sources and related human health risks. *Environ. Pollut* **2021,** 286, 117287.
33. Farnham, I. M.; Johannesson, K. H.; Singh, A. K.; Hodge, V. F.; Stetzenbach, K. J. Factor analytical approaches for evaluating groundwater trace element chemistry data. *Anal. Chim. Acta.* **2003,** 490, 123-138.
34. Gibbs, R. J., Mechanisms controlling world water chemistry. *Science.* **1970,** 170, 1088-1090.
35. Saikrishna, K.; Purushotham, D.; Sunitha, V.; Reddy, Y. S.; Brahmaiah, T.; Reddy, B. M.; Nallusamy, B. Deciphering groundwater quality, mechanisms controlling groundwater chemistry in and around Suryapet, Telangana, South India. *Total Environ. Res. Themes.* **2023,** 6, 100035.
36. Zhang, H. Y.; Han, X.; Wang, G. C.; Mao, H. R.; Chen, X. L.; Zhou, L.; Huang, D. D.; Zhang, F.; Yan, X. Spatial distribution and driving factors of groundwater chemistry and pollution in an oil production region in the Northwest China. *Sci. Total Environ.* **2023,** 875, 162635.